Evaluatins Impact Factor IBGM 2017 – 2018
IRAQI BULLETIN OF GEOLOGY AND MINING
Arcif: 0.0755
GIF: 0.936

Iraqi Bulletin of Geology and Mining *Vol.16, No.1, 2020* *p 63 – 77*

MINERALOGY AND STABLE SULFUR ISOTOPES OF THE SULFIDE MINERALIZATION IN THE KURADAWE AREA, MAWAT OPHIOLITE, KURDISTAN REGION, NORTHEASTERN IRAQ

Irfan O. Yara

Received: 12/ 04/ 2019, Accepted: 19/ 12/ 2019
Key words: Sulfide mineralization; Mineral chemistry; Stable sulfur isotopes; Mawat ophiolite; Kurdistan; Iraq

ABSTRACT

The study area is located in the Kuradawe village, 30 Km NE of Sulaimania City, in the east of the Kurdistan Region. The sulfide mineralization in the Kuradawe area is hosted by gabbro of the Mawat ophiolite. The petrographic study shows that the metagabbro has various microdomains, which contain different amphiboles and plagioclase. This indicates that the original magmatic rock and minerals were influenced by metamorphic overprint. The mineral assemblage of the metagabbro is represented by white amphibole, green amphibole, plagioclase, chlorite, quartz, epidote, pyrite, chalcopyrite, goethite and hematite. The metamorphic history can be subdivided into three stages (M1, M2, and M3). The first stage of metamorphism is recorded by the formation of green amphibole (tschermakite) replacing clinopyroxene. The second stage shows a decrease of temperature and pressure which resulted in the formation of white amphibole (tremolite); growing on the previous amphibole. While the late stage of metamorphism is recorded by the formation of chlorite and epidote. Three stages of mineralization are concluded from ore microscopic study: orthomagmatic stage, hypogene stage and supergene enrichment stage. Pyrite and chalcopyrite represent the main primary sulfide ore minerals. Hematite and goethite are the secondary ore minerals occurring as alteration products of the primary ore minerals. The $\delta^{34}S$ values of the sulfides range from + 7 to + 9 ‰, which indicate granitic composition for the mineralized fluids.

معدنية وتركيب نظائر الكبريت المستقرة في تمعدن كبريتيدات كوراداوي، إقليم كردستان، شمال شرق العراق

عرفان عمر يارا

المستخلص

تقع منطقة الدراسة في قرية كوراداوي، على بعد 30 كم شمال شرق مدينة السليمانية، في شرق إقليم كوردستان. الكبريتيدات المتمعدنة في كوراداوي مستضافة في صخور الغابرو ضمن أوفيوليت ماوات. تحتوي صخور الميتاغابرو على نطاقات ميكروية متنوعة، أذ تحتوي على أنواع مختلفة من ألامفيبولات والبلاجيوكليس وهذا يشير إلى أن الصخور الصهيرية والمعادن الأصلية متاثرة بعمليات تحول فوقية. التجمعات المعدنية للميتاغابرو تتمثل باالامفيبول الابيض والامفيبول الاخضر والبلاجوكليس والكلورايت والكوارتز والابيدوت والبايرايت والجالكوبايرايت والغوثايت والهيماتايت.

Department of Geology, University of Sulaimani, Sulaimani, Kurdistan Region, Iraq,
e-mail: irfan.mosa@univsul.edu.iq

يمكن تقسيم تاريخ التحول إلى المراحل M1 و M2 و M3. تم تسجيل المرحلة الأولى من التحول عن طريق تكوين الأمفيبول الأخضر (تجرماكيت) الذي حل محل الكلاينوبايروكسين. تظهر المرحلة الثانية انخفاضًا في درجة الحرارة والضغط مما أدى إلى تكوين الأمفيبول الأبيض (تريمولايت) وينمو على الأمفيبول السابق. بينما تم تسجيل المرحلة المتأخرة من التحول عن طريق تكوين الكلوريت والايبيدوت. تظهرمراحل تعاقب النشوء ثلاث مراحل من التمعدن. المرحلة الأولى الماغماتية ثم مرحلة الهيبوجين وتمثلها تمعدن الكبريتيد والمرحلة الثالثة هي مرحلة الاكسدة والاغناء وتتمثل بتمعدنات الأوكسيدات والهيدروكسيدات. يمثل البايرايت والجالكوبايرايت معادن الكبريتيدات الأساسية في حين تمثل معادن الهيماتايت والغوثايت معادن ثانوية تكونت بفعل عمليات الاكسدة للخامات المعدنية الكبرتيدية الأولية. تراوحت نظائر الكبريت ($\delta^{34}S$) بين ‰7 + و‰ 9 + مما يدل على ان مصدر المحاليل المعدنية ذو تركيب غرانيتي.

INTRODUCTION

The Zagros Orogen is subdivided into three parallel belts, these are; from northeast to southwest (Fig.1), the Tertiary Urumieh Dokhtar Magmatic Belt (Berberian and King 1981; Alavi, 1994), the Sanandaj-Sirjan Tectonic Zone (Alavi, 1994; Mohajjel and Ferguson, 2000; Mohajjel *et al*., 2003; Agard *et al*., 2005) and the Zagros Fold Belt (ZFB) (Stöcklin, 1968; Alavi, 1994; Mohajjel *et al*., 2003). The ZFB in the Kurdistan Region of Iraq can further be divided, from the northeast to the southwest, into three parallel NW – SE – trending structural domains, these are **i)** the Zagros Suture Zone (ZSZ), **ii)** the High Folded Zone, and **iii)** the Foot Hill Zone (Fig.1; Jassim and Goff 2006; Fouad, 2010).

The Kuradawe mineralization is located in northeastern Iraq, 30 Km northeast of Sulaimania City within the Mawat Ophiolite Complex, covering about 250 Km^2 within the Iraqi Zagros Zone (Jassim and Goff, 2006). It represents one of the Tethyan ophiolite complexes and part of croissant Ophiolite Belt (Ricou, 1971) which extends from Semail ophiolite of Oman to Troodos ophiolite of Cyprus passing through Iraq, Iran, Turkey and Syria (Fig.1). The Mawat ophiolite comprises the upper thrust sheet of the Mawat Nappe (Albian – Cenomanian) (Al-Mahaidi, 1975; Jassim and Goff 2006), and consists of 600 – 1000 m of basaltic and metabasalt intruded by plutonic complexes of ultrabasic pyroxenite, layered and massive gabbros, diorite, dolerite dikes and late-stage plagiogramite (Fig.2). Gabbro is the largest unit and includes banded gabbro, intruded from the east by coarse massive gabbros. This is followed by ultramafics (dunite and peridotite) that are variably serpentinized. The western contacts of the banded gabbro with the metavolcanics form a north-south trending shear zone, where the gabbro is highly deformed, brecciated and intruded by basic and acidic intrusions (Buday 1980, Buday and Jassim 1987, Zakaria 1992). The gabbro was thrust onto the metavolcanics during the final stages of solidification resulting in marginal shearing along the contact.

Copper occurrences are widespread all over the area of the Zagros Suture Zone, but only a few of them may be of economic interest. The distribution of mineral deposits in the northeastern part of Kurdistan is shown in Figure 3. Many of these occurrences are related to the serpentinized ultramafic rocks and gabbros of the Penjween, Mawat and Bulfat massifs. The Mawat area is characterized by a variety of metallic mineral deposits bearing Cu, Cr, and Mn (Fig.3). Copper ore mineralizations, mostly of the hydrothermal type, make up most of which in this area.

Williams (1948) reported the possibility to outline a zone of low-grade copper deposit near Waraz Police Post after which it was named the Copper Hill. The country rocks consist of diorite with an intrusion of quartz and brown schistose epidiosite. Williams (1948) referred in his report to the low-grade value of the copper in this occurrence. He considered the origin of the copper as the result of hydrothermal processes. He also reported that the copper content varies from 0.01% to 0.04%. Smirnov and Nelidov (1962) and Al-Hashimi

and Al-Mehaidi (1975) reported many copper mineralizations from the crush zone in gabbro SW of Kuradawe village and from granodiorites, pyroxenites and gabbros south of Konjrin village. The Cu-mineralization consists of chalcopyrite, pyrite, malachite and azurite, with Cu content between 2.84 and 23%. The main aim of this work is to study the mineralogy, mineral paragenesis and source of sulfur of the sulfide mineralization in the Kuradawe copper occurrence in the Mawat igneous complex, using petrographic, geochemical and stable isotopes methods.

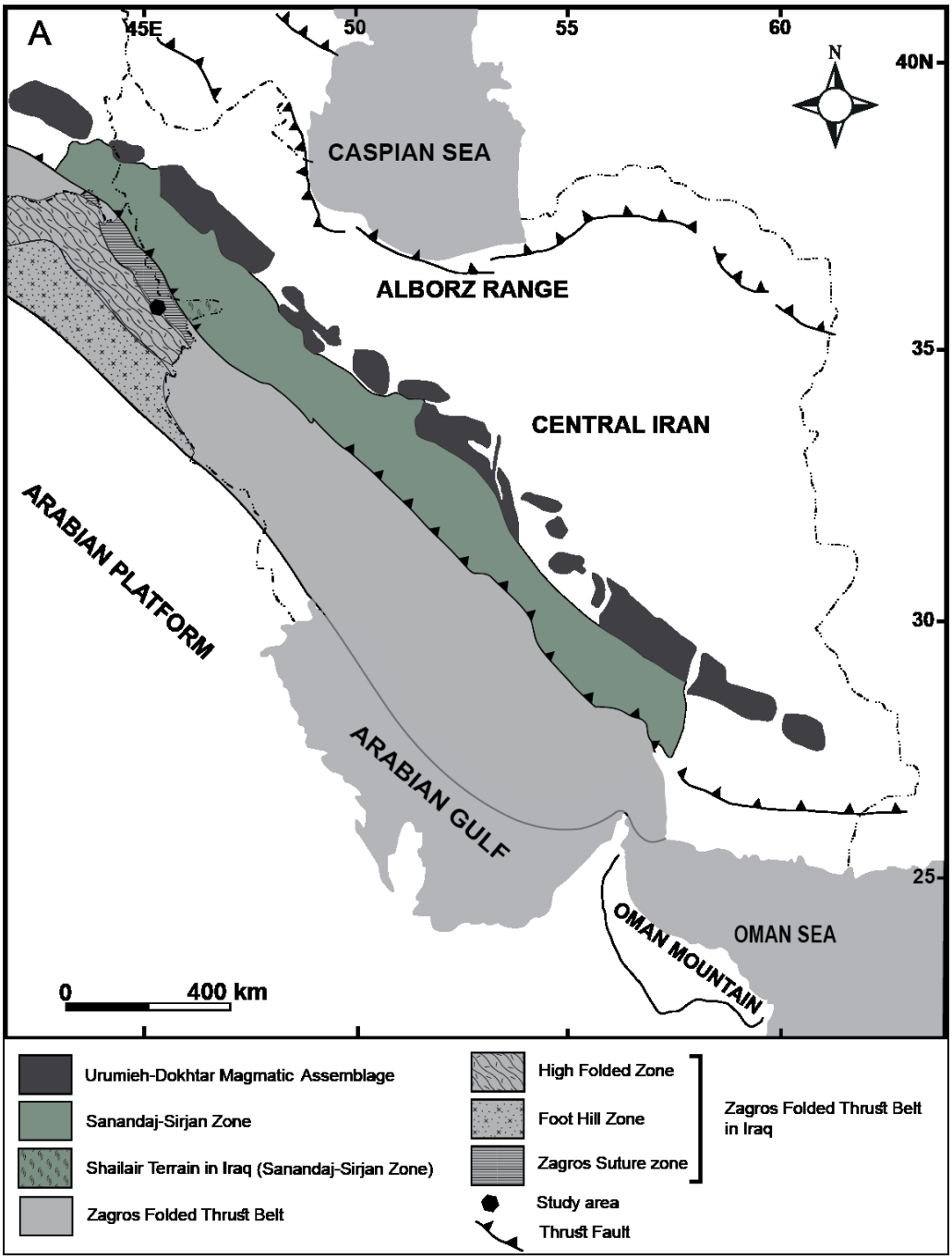

Fig.1: Zagros Orogenic Belt showing the main tectonic units and the location of the study area (after Jassim and Goff, 2006)

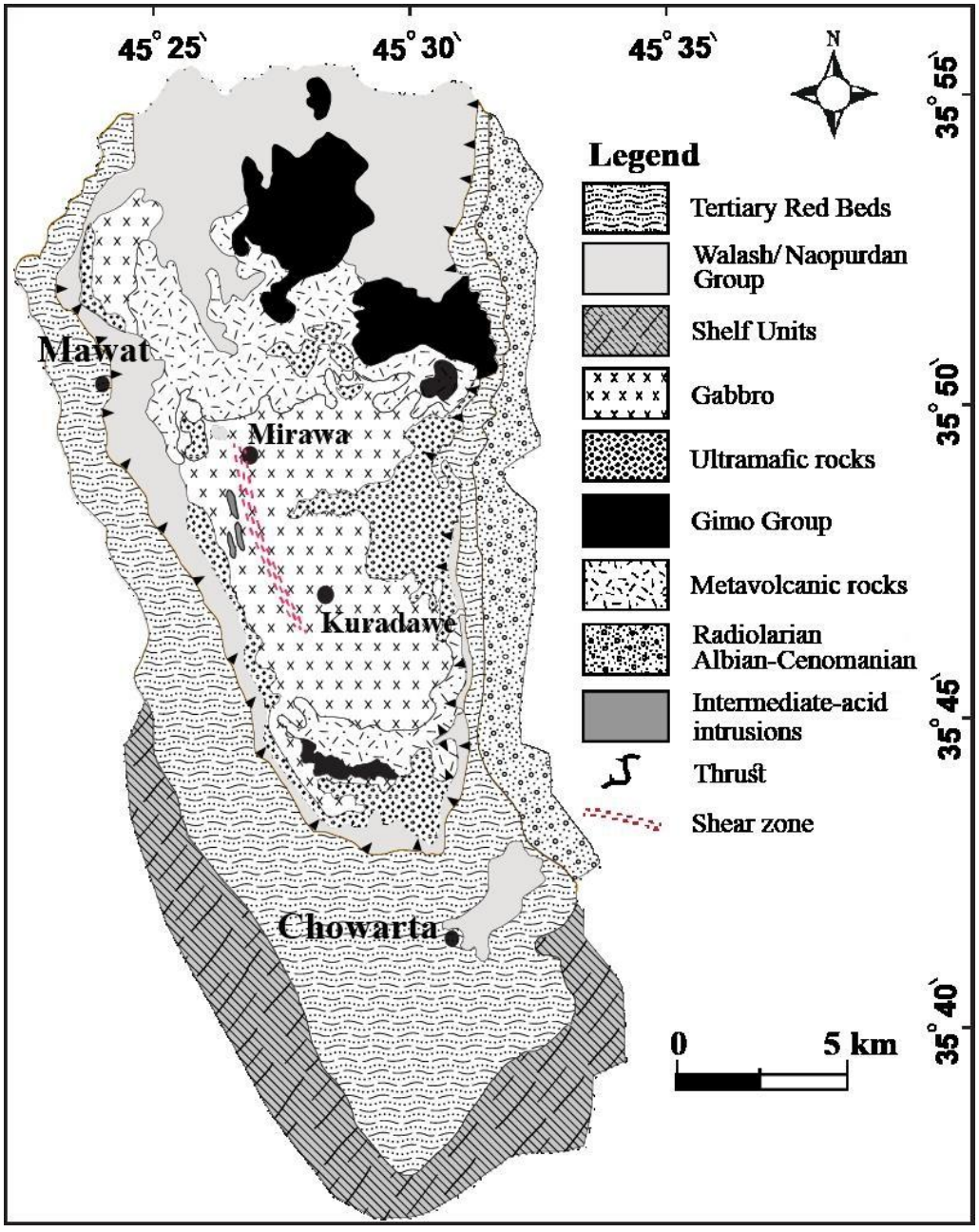

Fig.2: Geological map of the Mawat Ophiolite Complex, northeastern Iraq, (modified after Hama-Aziz, 2008)

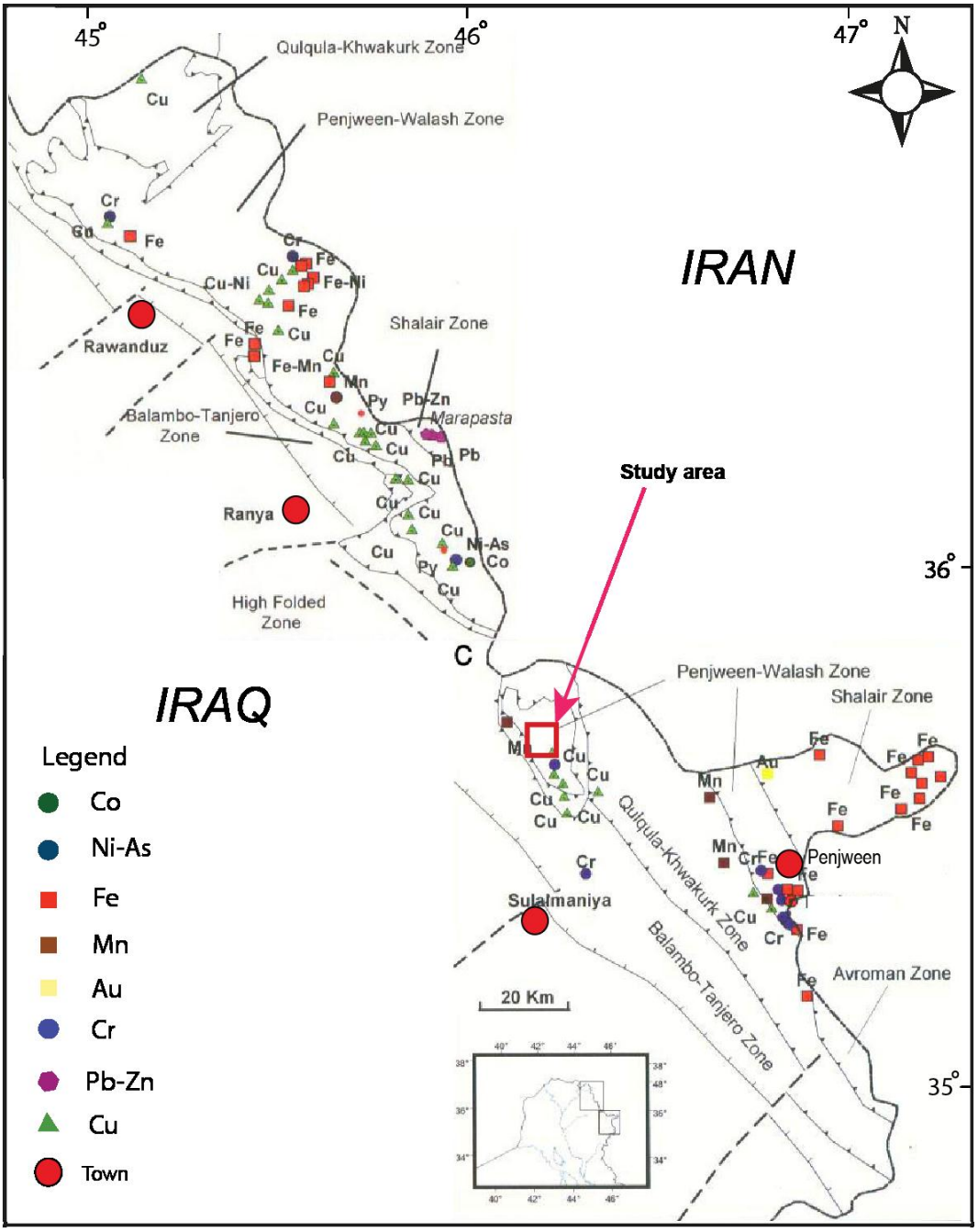

Fig.3: Distribution of metallic mineralizations in the Kurdistan Region, northeastern parts of Iraq (after Vanecek, 1972)

METHODOLOGY

- **Sampling and field observations**

The Kuradawe mineral occurrence lies in the Iraqi Zagros Suture Zone, at the south entrance of the Kuradawe village, where five meters of mineralization occur within the gabbro unit of the Mawat Ophiolite Complex. Fifteen surface samples of the mineralization and associated rocks were collected from the study area during two field trips. The samples are characterized by pale yellowish green weathered color in the weathered surface, but differ in the fresh surface where they appear grayish green with fine mineralization grains. The

fieldwork shows that the unit is moderately foliated metagabbro with irregularly scattered sulfide mineralization.

- **Petrography and mineral chemistry**

Fifteen thin sections were prepared for petrography and mineral chemistry investigation. All thin sections were studied by transmitting light polarizing microscope for texture and mineral identification. Four polished thin sections and three mount-polished sections were prepared for the mineralized samples. All polished sections were studied by reflected light polarizing microscope to identify texture and mineralogy. Scanning Electron Microscopy (SEM) equipped with Energy Dispersive Spectrometer (EDS) at TU Bergakademie Freiberg is used for microchemical analysis of the minerals constituents. The acceleration voltage used was 15 kV and the beam current was at 20 nA with the beam focused in a 2 µm diameter spot.

- **Sulfur stable isotope analysis**

Isotopic composition of three sulfide samples is determined at the isotope analytical facility of TU Bergakademie Freiberg. The results are reported as $\delta^{34}S$ values in per mil (‰), where: δ (‰) = [(R sample/ R standard) – 1] x 1000. The sulfur isotope composition of the analysed sulfides was determined using the elemental analyzer (Fisons Carlo Erba) coupled to mass spectrometer (CF-IRMS – Delta plus Thermo Quest-Finnigan) (e.g., Giesemann *et al*., 1994). The values were calibrated using one internal BaSO4 standard for drift correction and three international reference standards (IAEA-S-2, IAEA-S-3 and NBS 127) are used; to calibrate the instrument (Kornexl *et al*., 1999; Ding *et al*., 2001). All samples were analyzed at least in triplicate. The long-term reproducibility of sulfur isotopes was $\leq$ 0.3‰, although the internal error of three successive measurements was often smaller.

RESULTS

- **Petrography and Mineral chemistry**

The petrographic study shows that the samples mainly consist of amphibole (green and white), chlorite, pyrite, chalcopyrite, epidote, plagioclase, and quartz. Amphibole represents the most abundant mineral and it is formed from alteration of preexisting pyroxene. The most common feature of the studied samples is that the amphibole has formed, partially or completely overgrowing the clinopyroxene. Two types of amphibole are distinguished; **1)** white amphibole, formed due to intense deformation of preexisting pyroxene, and amphibole along their edges. It is more abundant than green amphibole and shows schistosity texture (Fig.4a). **2)** Green amphibole (tschermakite) occurs in subhedral to euhedral forms, and it shows parallel and subparallel pleochroism to the main foliation (Fig.4c). Petrographic study and chemical data show the different types of amphibole (Table 1). The amphiboles which are characterized by dark green color with pleochroism are tschermakite-hornblende to tschermakite (Fig.5). Actinolite and tremolite are pale green to colorless and characterized by fibrous texture (Fig.5).

Plagioclase occurs as anhedral grains. Two types of plagioclase are recognized; **a)** coarse grained with sutured boundary and undulose extinction (Pl I) Figure 4d and **b)** fine grained which is observed along the grain boundaries and fractures of the coarse plagioclase grains (Pl II) Figure 4d. The plagioclase hosted the fibrous amphibole which is formed as a deformation results (Fig.4d). In most samples the plagioclases are showing alteration to epidote (Fig.4d). Chemical data show that plagioclase is labradorite to bytownite (An_{67-77}) (Table 2).

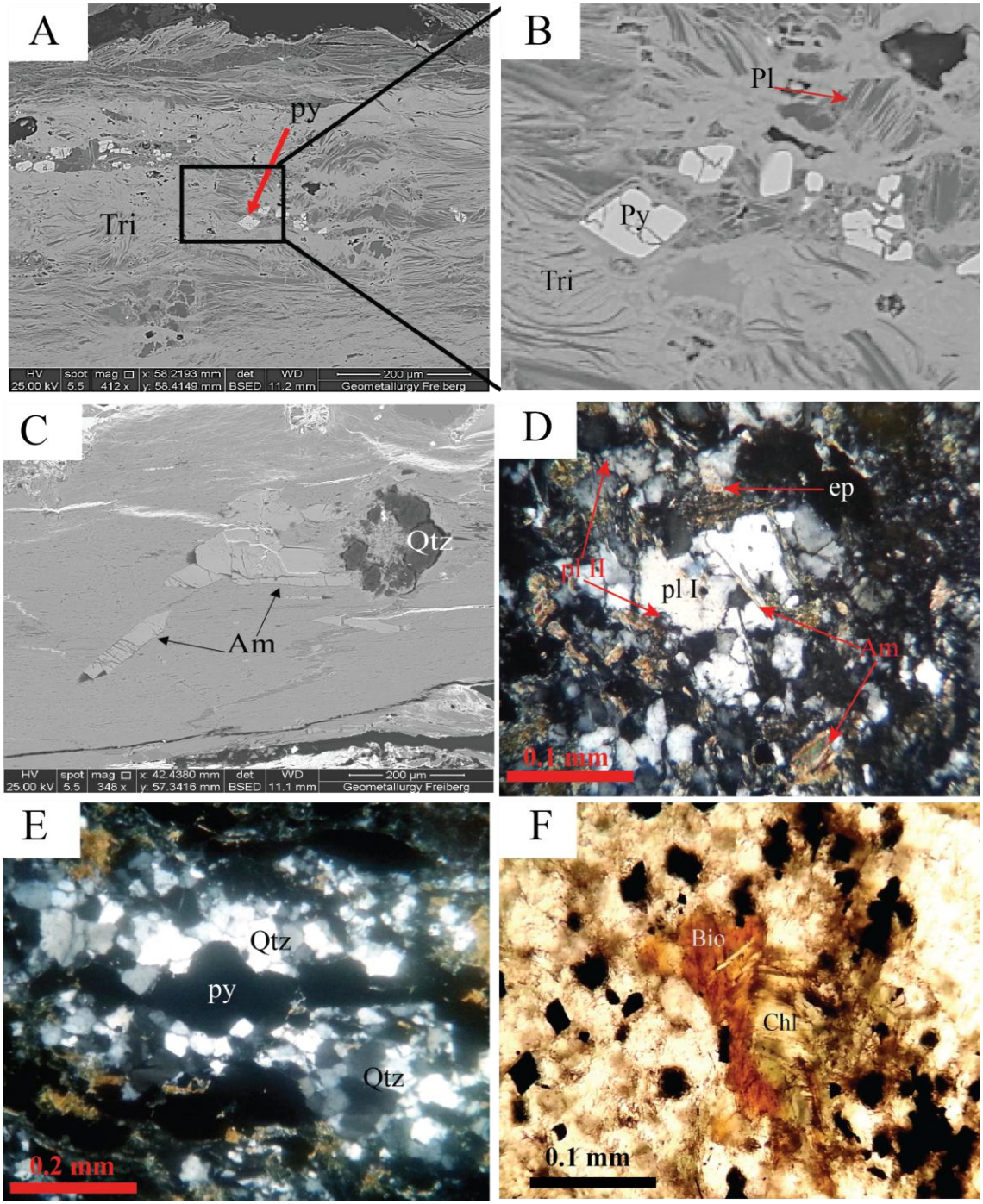

Fig.4: Photomicrographs of **A)** Trimolite showing mylonitic texture (back-scattered electron images), **B)** Euhedral pyrite formed by replacement growing and pushing aside the fibrous amphibole (back-scattered electron image), **C)** Back-scattered electron image showing subhedral to euhedral green amphibole, **D)** Plagioclase altered to epidote and fibrous amphibole growing into plagioclase, **E)** Oriented quartz (Qtz) aggregates, **F)** Biotite (Bio) and chlorite (Chl) showing two stages of deformation. (Tri) = Trimolite; (py) = pyrite; (Am) = amphibole; (pl) = plagioclase; (ep) = epidote; (Qtz) = quartz; (Bio) = biotite; (Chl) = chlorite

Table 1: Selected SEM analyses of amphibole, chlorite, and plagioclase from Kuradawe metagabbros

Sample No.	kur-1.1	kur 1-15	kur 1-14	kur 1-32	kur 1-35	kur-117 hb	kur-118 hb	kur 2-1	kur 1-66	kur 2-2…	kur 2-21	kur 2-23	kur 2-14	kur 1-36	kur-1
SiO_2	50.1	50.35	49.91	50.1	49.9	46.1	39.74	43.01	44.35	33.69	45.16	48.58	30.59	44.89	31.1
TiO_2	0.34	0.35	0.35	0.8	0.5	0.29	0.31	0.1	0.9	0.1	0	0.7	0	0.1	0.8
Al_2O_3	10.4	9.8	9.18	8.75	7.83	10.17	11.12	12.95	10.53	25.56	11.46	7.66	23.2	11.2	20.1
FeO	18.1	13.96	15.23	12.8	11.7	13.68	23.35	15.57	14.85	15.47	13.55	12.5	22.31	12.94	21.8
MnO	0.2	0.2	0.2	0.31	0.11	0.2	0.1	0	0.3	0	0.3	0.1	0.2	0.2	0.1
MgO	5.1	8.1	7.9	8.88	9.8	16.28	12.99	13.95	15.48	0	16.28	17.27	0	16.1	14.1
CaO	14.1	13.65	15.1	15.1	16.1	13.77	12.8	14.51	14.79	25.27	13.55	13.99	23.9	13.79	12.1
Na_2O	0.98	0.6	0.1	0.9	0.85	0	0.1	0	1.4	0.9	2.1	1.2	1.9	1.9	1.1
K_2O	0.15	0.32	0.13	1.8	1.75	0.1	0.12	0.13	2.3	1.3	1.3	2.3	0.9	0.82	0.3
Total	99.47	97.33	98.10	99.44	98.54	100.59	100.63	100.22	104.90	102.29	103.70	104.30	103.00	101.94	101.50
Si tot.	7.616	7.604	7.573	7.643	7.723	6.363	5.612	6.067	6.187	5.701	6.211	6.689	5.181	6.264	4.268
Si(T1)	3.616	3.604	3.573	3.643	3.723	2.363	1.612	2.067	2.187	1.701	2.211	2.689	1.181	2.264	0.268
Al tot.	1.863	1.744	1.642	1.573	1.428	1.654	1.851	2.153	1.731	5.097	1.858	1.243	4.631	1.842	3.251
Al IV	0.384	0.396	0.427	0.357	0.277	1.637	2.388	1.933	1.813	2.299	1.789	1.311	2.819	1.736	3.732
Al VI	1.479	1.348	1.215	1.216	1.152	0.018	-0.537	0.219	-0.082	2.798	0.069	-0.068	1.811	0.106	-0.48
Ti	0.039	0.040	0.040	0.092	0.058	0.030	0.033	0.011	0.094	0.013	0.000	0.072	0.000	0.010	0.083
Fe tot.	2.301	1.763	1.933	1.633	1.514	1.579	2.758	1.837	1.732	2.189	1.558	1.439	3.16	1.51	2.502
Fe^{+3}	0.000	0.000	0.000	0.000	0.000	1.469	0.000	1.284	0.000	0.000	0.000	0.383	0.000	0.825	4.144
Fe^{+2}	2.301	1.763	1.933	1.633	1.514	0.110	2.758	0.553	1.732	2.189	1.558	1.057	3.160	0.686	-1.64
Mn	0.026	0.026	0.026	0.040	0.014	0.023	0.012	0.000	0.035	0.000	0.035	0.012	0.029	0.024	0.012
Mg	1.156	1.824	1.787	2.019	2.261	3.35	2.735	2.933	3.219	0.000	3.338	3.545	0.000	3.349	2.885
Cr	0.000	0.000	0.000	0.000	0.000	0.000	0.000	0.000	0.000	0.000	0.000	0.000	0.000	0.000	0.000
Ca	2.296	2.209	2.455	2.468	2.67	2.036	1.937	2.193	2.211	4.581	1.997	2.064	4.337	2.062	1.779
Na	0.289	0.176	0.029	0.266	0.255	0.000	0.027	0.000	0.379	0.295	0.560	0.320	0.624	0.514	0.293
Na M_4	0.000	0.000	0.000	0.000	0.000	0.000	0.063	0.000	0.000	0.000	0.003	0.000	0.000	0.000	0.221
Na (A)	0.289	0.176	0.029	0.266	0.255	0.000	0.000	0.000	0.379	0.295	0.557	0.32	0.624	0.514	0.072
K	0.029	0.062	0.025	0.35	0.346	0.018	0.022	0.023	0.409	0.281	0.228	0.404	0.194	0.146	0.053
Vac.	0.682	0.763	0.945	0.384	0.399	0.982	0.978	0.977	0.212	0.424	0.215	0.276	0.182	0.34	0.876
X Mg (Fe_{2+})	0.334	0.508	0.48	0.553	0.599	0.968	0.498	0.841	0.65	0.000	0.682	0.77	0.000	0.83	2.321
Na + K (A)	0.318	0.237	0.055	0.616	0.601	0.018	0.022	0.023	0.788	0.576	0.785	0.724	0.818	0.660	0.124

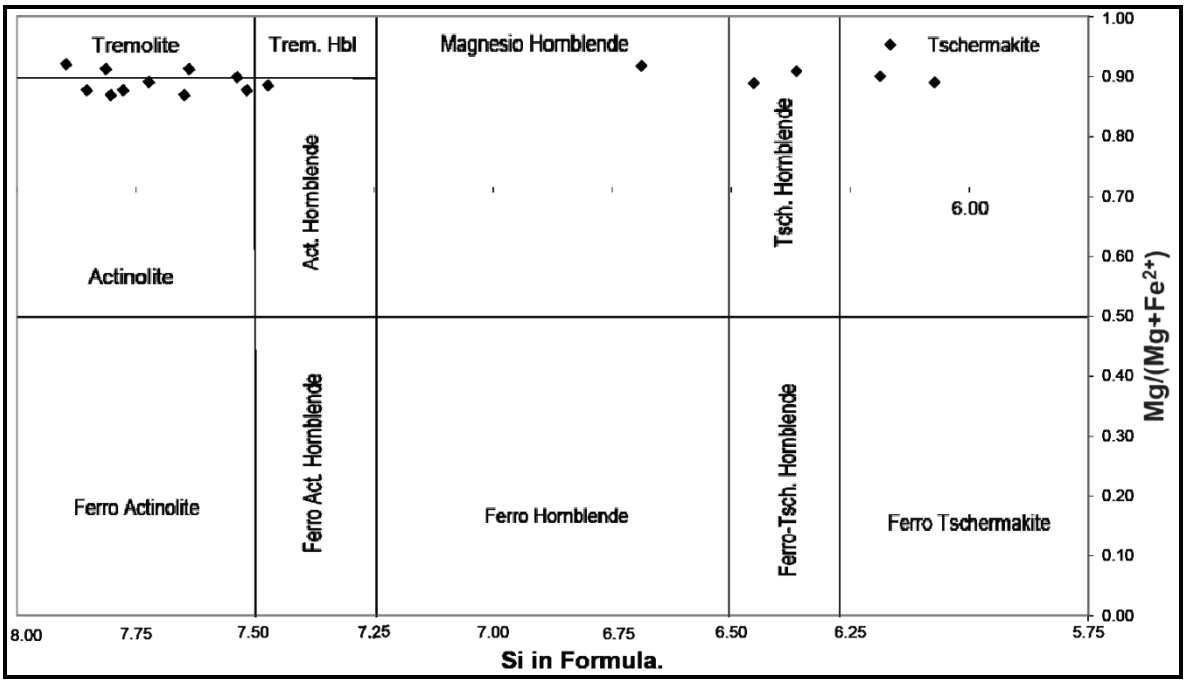

Fig.5: Compositional field and classification of the zoned Ca-amphiboles after Leake *et al*., (1997)

Table 2: Selected EDS analyses of chlorite, and plagioclase from Kuradawe metagabbros

	Chlorite							
Sample No.	**kur2-22**	**kur-39**	**kur1-43**	**kur1-24**	**kur2-13**	**kur1-55**	**kur1-56**	**kur1-57**
SiO_2	25.87	26.07	39.45	26.34	33.58	25.15	25.73	25.77
TiO_2	0.9	0.6	0.6	0.1	0.6	0.5	0.9	0.7
Al_2O_3	28.1	28.44	21.38	28.42	26.93	27.32	28.26	27.83
FeO	18.92	19.1	22.51	20.71	14.08	20.15	19.38	19.34
MnO	0.2	0	0	0	0.1	0	0	0.1
MgO	27.11	26.4	16.66	24.52	25.41	27.38	26.63	27.06
CaO	0	0	0	0	0	0	0	0
Na_2O	1.9	2	1.9	0.1	1.3	1.8	1.3	2.1
K_2O	1.8	1.2	1.5	0.3	1.1	1	1.6	1.9
	Chlorite	**Plagioclase**						
Sample No.	**kur1-65**	**kur-1.13**	**kur-119 my hb**	**kur1-23**	**kur-2.25**	**kur-2.36**	**kur-3.35**	**kur-5.11**
SiO_2	25.98	64.05	63.13	62.68	64.11	61.5	67.12	65.3
TiO_2	0.5	0	0	0	0.1	0.13	0.17	0.19
Al_2O_3	27.58	24.34	24.18	25.62	23.8	25.12	23.9	24.1
FeO	18.88	0	2.45	2.11	1.9	1.6	0.35	0.29
MnO	0.3	0	0	0	0	0	0	0
MgO	27.56	0	0	0	0	0	0	0
CaO	0	11.61	10.24	9.59	8.1	9.2	7.81	9.1
Na_2O	1.8	1.8	2.1	2.6	2.1	1.89	1.98	1.92
K_2O	2.1	0.2	0.12	0.34	0.23	0.13	0.13	0.11

Quartz occurs as aggregates and veins within the samples. Quartz aggregates display a strong crystallographic preferred orientation (Fig.4e); the long axes of quartz grains are arranged subparallel to parallel to the schistosity. The quartz is characterized by a sutured boundary, undulose extinction, deformation bands, and deformation lamella. Biotite is scarcely observed, grown parallel to the schistosity (Fig.4e), and thus representing the first stage of deformation (Fig.6). Chlorite is growing perpendicular to the biotite (Fig.4f).

- **Ore Mineralogy**

The studied samples are hosting disseminated sulfide and oxide minerals. Pyrite is the most dominant sulfide mineral, in addition to a minor amount of chalcopyrite. Pyrite is found in two types; **a)** Coarse grained pyrites which are characterized by cataclastic texture (Figs.7a and b) and sigma clast with strain shadow of amphibole and quartz (Fig.7c). Due to alteration, pyrite is partially replaced by goethite and hematite as rim replacement or island shape texture (Fig.7d). **b)** Fine grained pyrite occurs as aggregates of subhedral to euhedral grains. During deformation via replacement, the euhedral pyrite is grown by pushing aside the fibrous amphibole (Fig.4b). Chalcopyrite occurs in irregular form as inclusions in pyrite (Fig.7a), and it is the only copper-bearing mineral. Goethite and hematite are oxide minerals and they formed due to the oxidizing of the chalcopyrite and pyrite. They form rim, vein, and island shape replacement textures (Fig.7d).

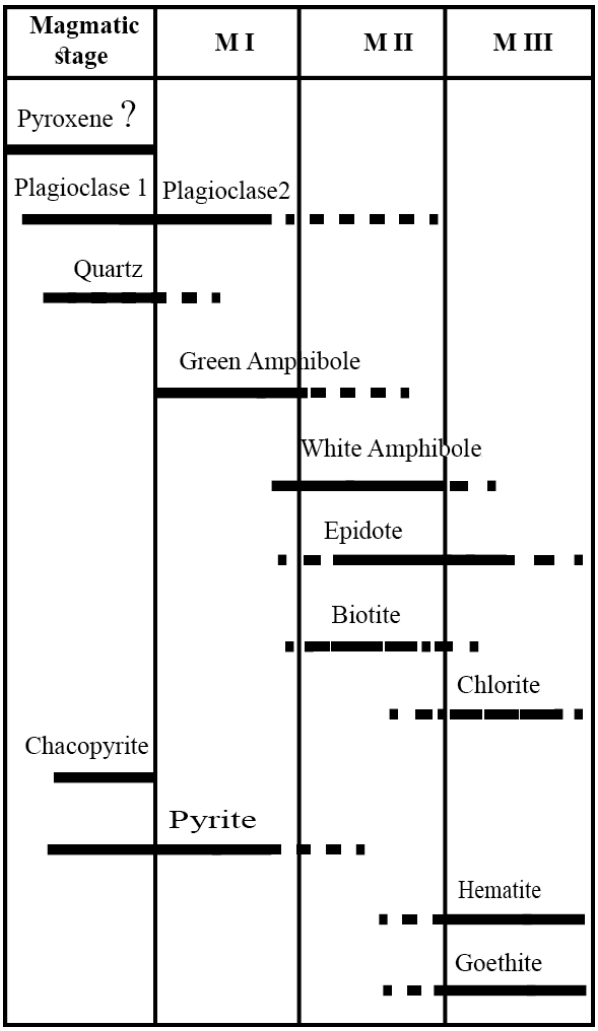

Fig.6: Mineral paragenesis in the Kuradawe metagabbro

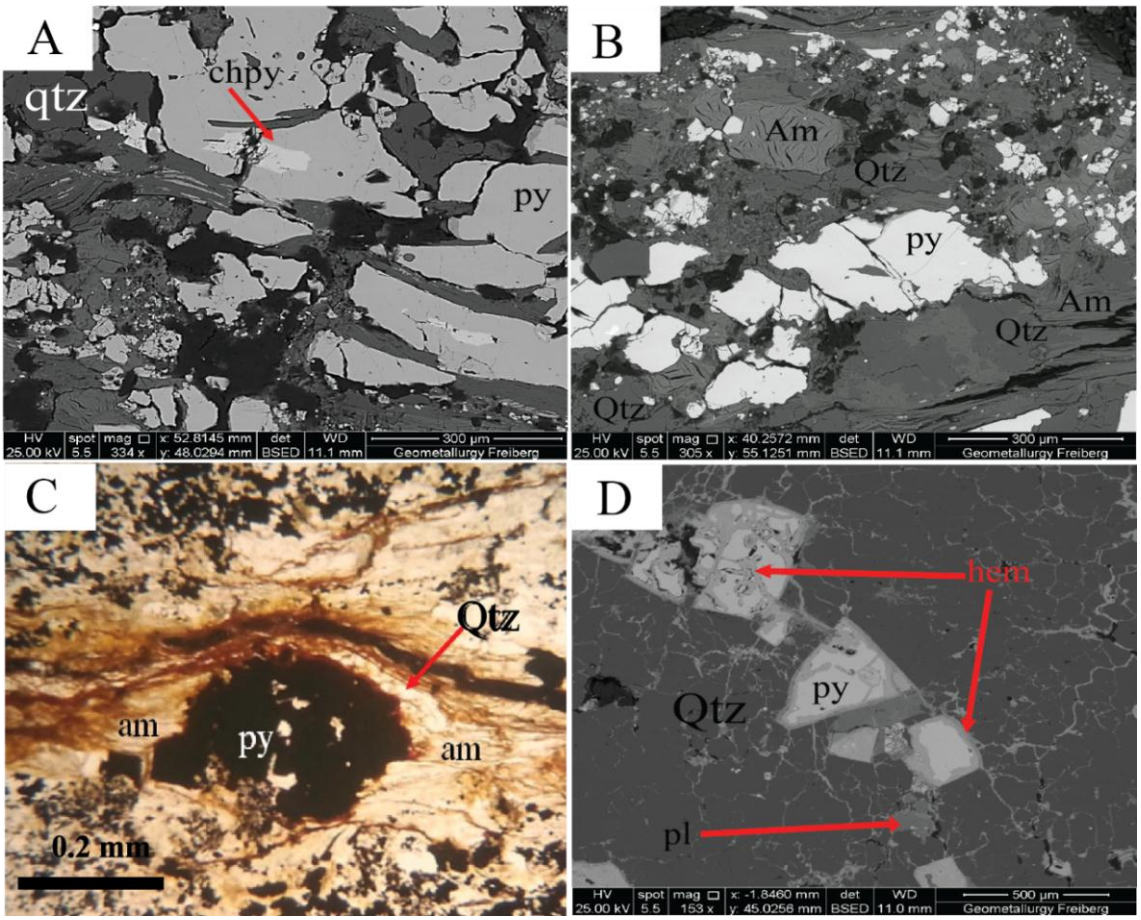

Fig.7: Photomicrographs of **A** and **B)** Back-scattered electron image showing catacalstic texture of pyrite and chalcopyrite as inclusions in pyrite, **C)** Coarse grained pyrite showing sigma clast with strain shadow of amphibole and quartz, **D)** Back-scattered electron image showing rim and island shape pyrite replacement by hematite. (chpy) = chalcopyrite; (py) = pyrite; (Am) = amphibole; (pl) = plagioclase; (Qtz) = quartz; (hem) = hematite

- **Stable sulfur isotope analysis**

The sulfur stable isotope composition ($\delta^{34}S$) of the sulfide minerals from three selected metagabbro samples were measured (Table 3). The $\delta^{34}S$ values of the sulfide minerals fall into a narrow range of +7.4 to +8.6 ‰, with an average of +7.9 ‰. The magmatic hydrothermal source hypothesis, which is primarily based upon the petrographic investigation, is supported by the sulfur isotope compositions (Fig.8). The $\delta^{34}S$ values of sulfides plot within the range of values assigned to granitic rock reservoir (Hoefs, 2009).

Table 3: Sulfur stable isotope $\delta^{34}S$ values of pyrite
(Measurement errors external reproducibility ≤ 0.3‰)

Sample No.	$\delta^{34}S$ [‰]
Ku2	8.6
Ku10	7.9
Ku 1	7.4

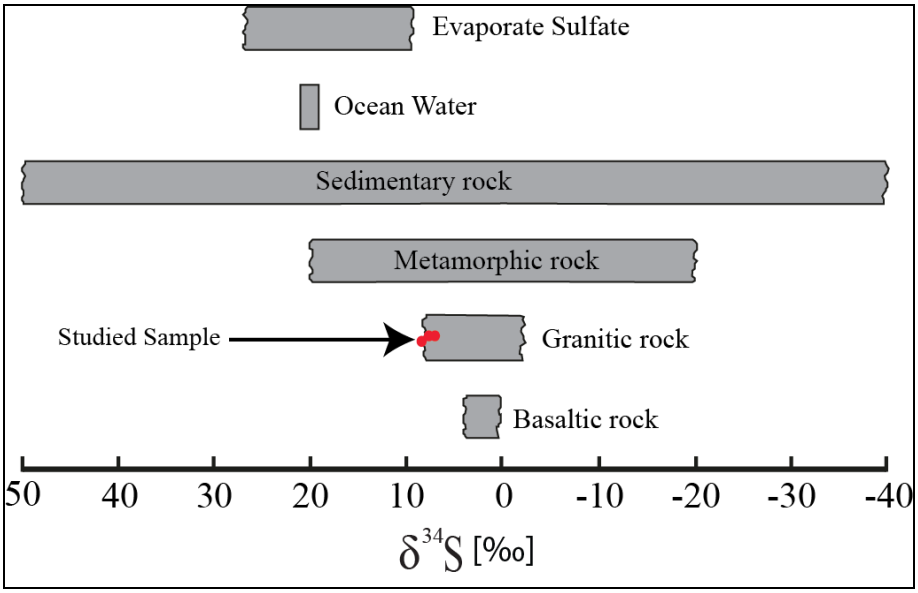

Fig.8: Sulfur isotope composition of pyrite from the Kuradawe metagabbro (red dots). The shaded areas represent the isotopic range of some geologically important sulfur reservoirs (after Hoefs, 2009)

DISCUSSION

Arabia – Eurasia continental collision recorded different stages of metamorphism. The investigated samples have been classified as "gabbro" (Al-Mahaidi, 1975). The petrographic investigation reveals that the pyroxene is absent in all samples as a result of metamorphism and replacement to green amphibole. Multiple amphibole equilibrium thermometers have shown that metabasite mineral assemblages with growth-zoned Ca-amphiboles manifest a high potential for pressure – temperature (P – T) reconstructions (e.g., Bégin and Carmichael, 1992; Triboulet, 1992; Schulz *et al*., 1995). Zoned amphiboles in magmatic and metabasic rocks are common and typical (e.g., Bégin and Carmichael 1992; Bachman and Dungan 2002; Schulz *et al*., 2001), and more rarely observed in metapelitic rocks (e.g., Vogl, 2003; Cruz, 2010). Rebay and Messiga (2007) concluded that the amphibole has various range of composition due to the high number of cation substitutions.

Metamorphic amphibole represents the major mineral in all the studied samples, suggesting persuasive effect of gabbroic rock metamorphism. Petrographic study and mineral chemical data show the zonation in the Ca-amphiboles where the grains show various Si content from core to rim (Fig.5). Green (tschermakite) and white (actinolite and tremolite) amphiboles are indicators of different stages of metamorphism. The first stage is recorded by tschermakite and in the second stage; actinolite and tremolite are replaced by green amphibole. The last stage is highlighted by chlorite overgrowth perpendicular on the main foliation of the rock (Fig.4f). In addition, the presence of pyrite showing sigma clast with strain shadow of amphibole and quartz points to area underwent shearing (Passchier and Trouw, 2005). Thus, this rock can be classified as metagabbro and the area as a sheared zone.

Ore microscopy shows that the samples are characterized by predominant sulfides and oxides ore minerals. They occur as disseminated and veinlets (Fig.4 and 7). The primary sulfide minerals include coarse subhedral and euhedral of pyrite and chalcopyrite as inclusions in pyrite (Fig.7a and b). The petrographic observations suggest that pyrite belongs to two stages: Pre-tectonic pyrite and Post-tectonic pyrite. The Pre-tectonic pyrite occurs in

coarse disseminated texture within the rock, showing catacalstic texture and sigma clasts (Fig.7a-c) (Yassin *et al*., 2015; Yara and Mohamad, 2018 and Yara, 2019). These textures indicate that the ore minerals are of orthomagamtic origin and they are derived from immiscible sulfide liquids (Ramdohr, 1981; Candela and Blevin, 1995; and Matthews *et al*., 1995; Musa, 2007). This type of pyrite was probably deformed during regional tectonic events of the Eurasian and Arabian plates obduction and subduction (Yara, 2019).

Post-tectonic pyrite occurs as euhedral and vein filing (Fig.4a and e), formed after the tectonic events (Musa, 2007; Yassin *et al*., 2015; Yara and Mohamad, 2018; and Yara, 2019). Such texture suggests that the source of pyrite is hydrothermal solution and this is emphasized by the sulfur isotope values with an average of +7.9 ‰. Rim, island shape and vein replacement of pyrite by oxide and hydroxide ore minerals represent the last stage of mineralization. Pyrite replacement by goethite is common under oxidizing condition as weathering product of iron-bearing minerals (Gilbert and Park, 1986; and Borg, 2004). This stage represents supergene enrichment stage of mineralization. Paragenetic sequence of ore mineral is given in figure 8 according to ore mineral texture relationship. Pyrite and chalcopyrite are the main ore minerals crystallized from immiscible sulfide liquid.

CONCLUSIONS

The studied samples are metagabbro within the sheared zone. The mineralogy of the Kuradawe Cu-mineralization is sulfide minerals including pyrite and chalcopyrite as primary minerals and hematite and goethite as secondary minerals. The petrographic study suggests that the ore minerals and the host rocks suffered the same metamorphic history. Paragenetic sequence show three stages of mineralization; orthomagmatic, hypogene and supergene. The $\delta^{34}S$ data of the sulfide minerals reveal that the source of the mineralized fluids is of granitic composition.

REFERENCES

Agard, P., Omrani, J., Jolivet, L. and Mouthereau, F., 2005. Convergence history across Zagros (Iran): Constraints from collisional and earlier deformation. International Journal of Earth Sciences, Vol.94, p. 401 – 419.

Alavi, M., 1994. Tectonics of the Zagros orogenic belt of Iran: new data and interpretations. Tectonophysics, Vol.229, p. 211 – 238.

Al-Hashimi, A.R. and Al-Mehaidi, H.M., 1975. Cu-Ni-Cr dispersion in Mawat ophiolite complex, NE Iraq. Jour. Geol. Soc. Iraq, Spec. Issue, 37pp.

Al-Mehaidi, H.M., 1975. Tertiary nappes in Mawat range, NE Iraq. Jour. Geol. Soc. Iraq, Vol.7, p. 31 – 44.

Bachman, O. and Dungan, M.A., 2002. Temperature induced Al-zoning in hornblendes of the Fish Canyon magma, Colorado. American Mineralogist, Vol.87, p. 1062 – 1076.

Bégin, N.J. and Carmichael, D.M., 1992. Textural and compositional relationships of Ca-amphiboles in metabasites of the Cape Smith Belt, Northern Québec: Implications for a miscibility gap at medium pressure. Journal of Petrology, Vol33, p. 1317 – 1343.

Berberian, M. and King, G.C.P., 1981. Towards a paleogeography and tectonic evolution of Iran. Canadian Journal of Earth Sciences, Vol.18, p. 210 – 265.

Borg, G., 2004. Metallogenesis of non-sulfide zinc deposits. Southern Namib Desert, Namibia. Petrogenic and Lagerstatten for chung, Vol.5, p. 1 – 4.

Buday, T., 1980. The regional geology of Iraq. Volume I, Stratigraphy and Paleogeography edt. By Kassab, I.M. and Jassim, S.Z., Dar Al-Kutib publishing house, Mosul, Iraq, 445pp.

Buday, T. and Jassim, S.Z., 1987. The Regional Geology of Iraq. Vol.2, Tectonism, Magmatism, and Metamorphism. Geol. Surv. Min. Inv. Baghdad, 352pp.

Candela, P. and Blevin, P., 1995. Physical and chemical magmatic controls on the size of magmatic-hydrothermal ore deposits: Giant ore deposits II. Queen's University, p. 2 – 42.

Cruz, M.D.R., 2010. Zoned Ca-amphibole as a new marker of the Alpine metamorphic evolution of phyllites from the Jubrique unit, Alpujárride Complex, Betic Cordillera. Spain Mineralogical Magazine, Vol.74, p. 773 – 796.

Ding, T., Valkiers, S., Kipphardt, H., DeBievre, P., Taylor, P.D.P., Gonfiantini, R. and Krouse, R., 2001. Calibrated sulfur isotope abundance ratios of three IAEA sulfur isotope reference materials and V-CDT with reassessment of the atomic weight of sulfur. Geochim. Cosmochim. Acta, Vol.65, p. 2433 – 2437.

Fouad, S.F., 2010. Tectonic Map of Iraq, Scale 1: 1000 000, 3rd; GEOSURV, Baghdad, Iraq.

Giesemann, A., Jäger, H.J., Norman, A.L., Krouse, H.R and Brand, W.A., 1994. On-line sulfur isotope determination using an elemental analyzer coupled to a mass spectrometer. Anal. Chem., Vol.66, p. 2816 – 2819.

Gilbert, J.M. and Park, C.F., 1986. The geology of ore deposits. Freeman and company, New York, 958pp.

Hama-Aziz, N.R., 2008. Petrogenesis, evolution, and tectonics of the serpentinites of the Zagros suture zone, Kurdistan Region, NE Iraq. Unpublished Ph.D. Thesis, Sulaimani University, Sulaimania, Kurdistan Region, Iraq, 250pp.

Hoefs, J., 2009. Stable isotope geochemistry. Springer, Heidelberg

Jassim, S.Z. and Goff, J.C., 2006. Geology of Iraq. Parague and Moravian Museum Brno. 341pp.

Kornexl, B.E., Gehre, M., Höfling, R. and Werner, R.A., 1999. On-line δ18O measurement of organic and inorganic substances. Rapid Commun. Mass Spectrom. Vol.13, p. 1685 – 1693.

Leake, B.E., Woolley, A.R., Arps, C.E.S., Birch, W.D., Gilbert, M.C, Grice, J.D., Hawthorne, F.C., Kato, F.C., Kisch, H.J., Krichovichev, V.G., Linthout, K., Laird, J., Mandarino, J.A., Maresch. W.V., Nickel, E.H., Rock, N.M.S., Schumacher, J.C., Smith, D.C., Stephenson, N.C.N., Ungaretti, L., Whittaker, E.J.W. and Youzhi, G., 1997. Nomenclature of amphiboles: report of the subcommittee on amphiboles of the International Mineralogical Association, Commission on New Minerals and Mineral Names. American Mineralogist, Vol.82, p. 1019 – 1037.

Matthews, S., Sparks, S. and Gadeweg, M., 1995. The relationships between magma mixing and volatiles behavior at Lascar Volcano, northern Chile; Significance for formation copper sulphide and magnetite-apatite ore bodies; Giant Ore Deposite II, Queen's University Kigstone, p. 146 – 181.

Mohajjel, M. and Fergusson, C.L., 2000. Dextral transpression in Late Cretaceous continental collision, Sanandaj – Sirjan zone, western Iran. Journal of Structural geology, Vol.22, No.8, p. 1125 – 1139.

Mohajjel, M., Fergusson, C.L. and Sahandi, M.R., 2003. Cretaceous – Tertiary convergence and continental collision, Sanandaj – Sirjan zone, western Iran. Journal of Asian Earth Sciences, Vol.21, No.4, p. 397 – 412.

Musa, E.O., 2007. Petrography, Geochemistry and Genesis of Copper-Iron Mineralization and Associated Rocks in Waraz Area, Sulaimania, NE Iraq. Unpublished M.Sc. Thesis, University of Baghdad, Baghdad, 155pp.

Passchier, C. and Trouw, R.A.J., 2005. Microtectonics. 2nd. Springer, Berlin Heidelberg, 366pp.

Ramdohr, P., 1981. The Ore Minerals and Their Intergrowth. Pergamon Press., New York, 1202pp.

Rebay, G., Messiga, B., 2007. Prograde metamorphic evolution and development of chloritoid-bearing eclogitic assemblages in subcontinental metagabbro (Sesia – Lanzo zone, Italy). Lithos, Vol.98, p. 275 – 291.

Ricou, L.E., 1971. Le Croissant Ophiolitique Peri-Arab: Une ceinture de nappes mises en place an cretace superieur. Rev. Geogr. Phys. Geol. Dyn., Vol 13, p 327 – 349.

Schulz, B., Triboulet, C. and Audren, C., 1995. Microstructures and mineral chemistry in amphibolites from the western Tauern Window (Eastern Alps), and P-T-deformation paths of the Alpine greenschist-amphibolite facies metamorphism. Mineralogical Magazine, Vol.59, p. 641 – 659.

Schulz, B., Triboulet, C., Audren, C., Pfeifer, H.R. and Gilg, A., 2001. Two-stage prograde and retrograde Variscan metamorphism of glaucophane-eclogites, blueschists and greenschists from Ile de Groix (Brittany, France). International Journal of Earth Sciences, Vol.90, p. 871 – 889.

Smirov, V.A., Nelidov, V., 1962. Report on 1: 200 000 prospecting correlation of Sulaimaniya, Chwarta, Penjwin area, Carried out in (1962). GEOSURV, int. rep. no. 290.

Stöcklin, J., 1968. Structural history and tectonics of Iran: a review. AAPG Bull., Vol.52, No.7, p. 1229 – 1258.

Triboulet, C., 1992. The (Na – Ca) amphibole – albite – chlorite – epidote – quartz geothermobarometer in the system S – A – F – M – C – N – H_2O. 1. An empirical calibration. J Metamorph Geol., Vol.10, p. 545 – 556.

Vanecek, M., 1972. The principal metallogenic features of Iraq. Acta Universitatis Carolinne-Geologica, Vol.3, p. 237 – 252.

Vogl, J.J., 2003. Thermal-baric structure and P – T history of the Brooks Range metamorphic core, Alaska. Journal of Metamorphic Geology, Vol.21, p. 269 – 284.

Williams, W.R., 1948. Mineral survey of mountains of north Iraq. GEOSURV, int, rep. no. 133.

Yara, I., 2019. Copper mineralization in selected areas of Kurdistan region, Iraq: A review on mineralogy on mineralogy and geochemistry. Iraqi Bulletin of Geology and Mining, Special issue, Vol.8, p. 41 – 63.

Yara, I. and Mohammad, Y., 2018. Iron-copper mineralization associated with metagabbro in Mirawa Village, Kurdistan Region, Northeastern Iraq, Journal of Zankoy Sulaimani, Vol.20, No.2, p. 95 – 108.

Yassin, A.T., Alabidi, A.J., Hussain, M.L., Al-Ansari, N. and Knutsson, S., 2015. Copper ores in Mawat Ophiolite Complex (Part of ZSZ), NE Iraq. Natural Resources, Vol.6, p. 514 – 526.

Zakaria, M.B.M., 1992. Petrology and geochemistry of the southern part of Mawat ophiolite complex, northeastern Iraq. Unpubl. M.Sc. Thesis, University of Mosul.

About the author

Dr. Irfan O.M. Yara, Lecturer at the University of Sulaimani, Iraq. He teaches undergraduate and postgraduate courses. Yara received his B.Sc. degree in Geology from Sulaimani University, Iraq in 2002 and M.Sc. degree in Petrology from the University of Baghdad in 2007. He got his Ph.D. degree in Geochemistry and Ore Geology from TU Bergakadimie Freiberg – Germany in 2014. He taught at the University of Kurdistan Hawler (2015 – 2018) as visiting lecturer. Yara published 8 papers in petrology, ore mineralization, mineralogy and geochemistry in Iraqi and regional journals.

e-mail: irfan.mosa@univsul.edu.iq
Mailing address: University of Sulaimani, Sulaimania City, Kurdistan Region, Iraq